Neuro-Oncology

Prognostic value of MIB-1, p53, epidermal growth factor receptor, and INI1 in childhood chordomas

Rajni Yadav, Mehar Chand Sharma, Prit Benny Malgulwar, Pankaj Pathak, Elanthenral Sigamani, Vaishali Suri, Chitra Sarkar, Amandeep Kumar, Manmohan Singh, Bhawani Shankar Sharma, Ajay Garg, Sameer Bakhshi, and Mohammed Faruq

Department of Pathology, All India Institute of Medical Sciences, New Delhi, India (R.Y., M.C.S., P.B.M., P.P., E.S., V.S. C.S.); Department of Neurosurgery, All India Institute of Medical Sciences, New Delhi, India (A.J., M.S., B.S.S.); Department of Neuroradiology, All India Institute of Medical Sciences, New Delhi, India (A.G.); Department of Medical Oncology, All India Institute of Medical Sciences, New Delhi, India (S.B.) Genomics and Molecular Medicine, Institute of Genomics and Integrative Biology – Council of Scientific and Industrial Research (IGIB-CSIR), New Delhi, India (M.F.)

Corresponding author: Mehar Chand Sharma, MD, Department of Pathology, All India Institute of Medical Sciences, New Delhi 110029, India (sharmamehar@yahoo.co.in).

Background. Chordomas are slow-growing tumors and most commonly involve the sacrum and clivus. Multiple recurrences are frequent. Childhood chordomas are rare and often show exceptionally aggressive behavior, resulting in short survival and a high incidence of metastatic spread.

Objective. This study examined the histologic features and immunohistochemical profile of pediatric chordomas and compared them with their adult counterparts.

Methods. Nine pediatric and 13 adult cases were included in the study. Childhood chordomas were classified into conventional, atypical, and poorly differentiated types. Immunohistochemistry was performed for cytokeratin, epithelial membrane antigen, vimentin, S100, brachyury, p53, INI1, epidermal growth factor receptor (EGFR), and CD117. Cytogenetic analyses were performed in a subset of tumors for SMARCB1/INI1 locus on 22q chromosome by fluorescent in situ hybridization (FISH) and analysis of the SMARCB1/INI1 gene sequence.

Results. All tumors showed expression of cytokeratin, epithelial membrane antigen, S100, vimentin, brachyury, and EGFR. Atypical morphology, p53 expression, higher MIB-1 labelling index (LI), and INI1 loss were more frequently seen in pediatric chordomas as compared with adults. None of the tumors showed CD117 expression. No point mutation in the SMARCB1/INI1 gene was noted in the tumors examined; however, 4 pediatric and 1 adult chordoma showed loss of this locus on FISH analysis.

Conclusions. A subset of pediatric chordomas with atypical histomorphologic features needs to be identified, as they behave in an aggressive manner and require adjuvant therapy. Pediatric chordomas more frequently show p53 expression, INI1 loss, and higher MIB-1 LI as compared with adults, whereas EGFR expression is common to both.

Keywords: chordoma, clivus, EGFR, INI1, pediatric.

Chordomas are infiltrative neoplasms of bone that arise in the axial spine, most commonly involving the sacrum and clivus.[1,2] They account for 1%–4% of primary bone tumors.[3,4] These tumors are believed to arise from notochordal remnants. A few recent studies suggest an origin from intraosseous benign notochordal cell tumors.[5,6] Most cases occur in adults, with a peak incidence in the sixth and seventh decades.[7] Males are affected more frequently than females. Chordomas are rare in the pediatric population, and fewer than 5% occur in patients younger than 20 years of age.[8] In children, chordomas most frequently occur in the skull base.[9,10]

Although usually slow-growing, chordomas are extremely difficult to eradicate by surgical and adjuvant means. Multiple recurrences cause considerable mortality. Five- and 10-year survival rates vary between 70%–80% and 30%–40%, respectively.[11,12] Skull-base chordomas are not amenable to complete surgical

excision due to their inaccessibility and close proximity to vital structures. Consequently, they are treated with postoperative adjuvant radiation therapy using either conventional or proton-beam radiation.[5] Pediatric chordomas often show exceptionally aggressive behavior with short survival and a high incidence of metastatic spread.[9,13] Although pediatric chordomas are known to occasionally have unusual morphologic features, their genetic alterations have not been studied in detail. The current study examines the histologic features and immunohistochemical profile of pediatric chordomas and compares them with their adult counterparts.

Materials and Methods

All pediatric chordoma cases diagnosed during a period of 5 years in the Department of Pathology at All India Institute of Medical Sciences (one of the largest tertiary care centers in northern India) were included in the study, and the slides were retrieved from archives of the department. The tumor tissue had been fixed in 10% neutral buffered formalin, routinely processed, and paraffin-embedded. Hematoxylin and eosin (H&E) stained sections were reviewed by 3 independent neuropathologists (RY, MCS, and CS), and consensus diagnoses were made. Tumors were evaluated for architectural pattern, degree of cellularity, amount and character of stroma, presence of chondroid morphology, cytologic atypia, mitotic count, percent tumor necrosis, and presence or absence of vascular invasion. Cytologic atypia was defined as pleomorphic hyperchromatic nuclei and/or markedly vesicular nuclei with macronucleoli. Tumors were defined as cellular when composed of confluent sheets of tumor cells with no myxoid stroma.

Immunohistochemistry

Immunohistochemical studies were performed on 5-micron thick formalin-fixed, paraffin-embedded tumor sections using antibodies directed against pan-cytokeratin (NeoMarker; dilution 1:100), epithelial membrane antigen (Dako; dilution 1:100), vimentin (Novocastra; dilution 1:100), S-100 (Dako; dilution 1:1500), MIB-1 (Dako; dilution 1:200), brachyury (Santa Cruz Biotechnology; dilution 1:200), p53 (DO, 1clone) (Santa Cruz Biotechnology; dilution 1:100), epidermal growth factor receptor (EGFR) (Dako, dilution 1:100), INI1 (Cell Marque; dilution 1:100), and CD117 (Dako; dilution 1:100). In addition, immunostaining for glial fibrillary acidic protein (GFAP) (Dako, dilution 1:1000), smooth muscle actin (Dako, dilution 1:50), desmin (Dako; dilution 1:50), chromogranin (Neomarker; dilution 1:100), and synaptophysin (Neomarker; dilution 1:200) was also performed in cases with atypical morphology. Labeled streptavidin biotin kit (Dako) was used as a detection system. Antigen retrieval, when required, was performed in a microwave oven. MIB-1 labeling index (LI) was calculated in the highest proliferating areas as percentage of labeled nuclei per 1000 cells. For p53, strong nuclear positivity of good intensity in >10% of cells was considered as positive. Endothelial cells of blood vessels in the tumor acted as internal positive control for INI1. To test the specificity of brachyury, immunostaining for brachyury was performed in 18 malignant rhabdoid tumors (3 renal and 15 central nervous system atypical teratoid/rhabdoid tumors [AT/RTs]).Clinical parameters, including clinical presentation, duration of symptoms, site of tumor, and imaging findings were noted from the records.

Tissue Procurement and DNA Extraction

Four tumors of childhood and 1 of adult with adequate material in the blocks and loss of INI1 expression on immunohistochemistry (IHC) was taken for DNA extraction. Those sections where the flanking H&E sections showed tumor content >80% with minimal necrosis and without normal tissue were used for DNA extraction. Eight serial sections of 10 microns were collected from each formalin-fixed, paraffin-embedded block. We used the Recover All™ Total Nucleic Acid Isolation kit (Ambion) to extract DNA per manufacturer's instructions.

DNA Sequencing

PCR amplification was carried out for all 9 exons of INI gene, with primers used in an earlier study by Kraus et al.[14] PCR amplification of 1–9 exons was performed in a 10 μL reaction mixture containing 50 ng of tumor DNA, 1 μL of 10X PCR buffer, 0.8 μL of 10 mM dNTPs, 0.25 μL each of forward and reverse primers, and 0.2 μL of AmpliTaq Gold PCR Master Mix (Applied Biosystems). Initial denaturation was carried out at 95°C for 5 minutes. This was followed by 35 cycles of amplification consisting of denaturation at 95°C for 1 minute, annealing at 57°C for 45 seconds, and extension at 72°C for 2 minutes. Bidirectional sequencing was performed using ABI 3730 sequencer (Applied Biosystems).

Fluorescent in Situ Hybridization Analysis

Fluorescent in situ hybridization analysis (FISH) was performed on 4 childhood chordomas with INI1 loss that had sufficient paraffin-embedded tissue samples. Four adult chordomas without INI1 loss and 1 with INI1 loss were also studied for comparison. Dual color, dual fusion bcr/abl translocation probes for reciprocal t(9;22)(q34;q11.2) locus (Vysis, Abbott Laboratories) were used. Sections were deparaffinized by immersing 3 times in xylene for 10 minutes each, followed by two 3 minute immersions in 100% ethanol. Following rinsing in water, target retrieval was achieved using citrate buffer, pH 6.0, and boiling in a microwave oven for 20 minutes. Slides were exposed to 0.04% pepsin (P-7000; Sigma-Aldrich) digestion for 30 minutes at 37°C, fixed, and dehydrated. Probe mixture (10 μL per slide) was applied on each section. Simultaneous probe/specimen denaturation was performed at 73°C for 5 minutes with subsequent overnight incubation at 37°C in Thermobrite TM hybridization chamber (Vysis, bbott Laboratories). The sections were washed the next day in 2X SSC (2 min at 73°C) followed by 0.5X SSC (2 min at room temperature), counterstained with 4,6-diamidino-2-phenylindole (Abbott Laboratories), and visualized under a fluorescent microscope. Signals were scored in at least 200 nonoverlapping intact nuclei, and the number of test (red) and control (aqua) signals was noted. Nuclei with 2 test and 2 control signals were regarded as normal. Cases with one test signal in > 40% of cells were considered to have deletion of 22q.

Results

Over a period of 5 years, 10 childhood chordomas were diagnosed in our department, of which one was excluded because of insufficient material. For comparison, 13 adult chordomas, which were diagnosed in the last 2 years, were included. Tumors that showed expression for brachyury were included in the study.

Pediatric Group

The pediatric group consisted of 9 patients, 2 of whom had recurrent tumors. Clinical parameters, histopathologic features, and immunohistochemical profile are summarized in Table 1. Ages of the patients ranged from 2–18 years with a mean age of 8.1 years. There were 7 males and 2 females with a male-to-female ratio of 3.5:1. The most common location was clivus (7 cases) followed by nasal cavity in one case and posterolateral neck (cervical spine) in one case. Clinical signs and symptoms varied from neck pain, headache, gait instability, weakness in the limbs, nasal obstruction, and proptosis to diminution and loss of vision. The radiologic findings included low or isosignal intensity on computed

Table 1. Clinical, histopathologic and immunohistochemical features of pediatric chordomas

Case no	1	2	3	4	5	6	7	Recc	8	9	Recc
Age(years)/Sex	7/M	8/F	4/M	10/M	12/M	6/M	18/M		2/F	6/M	
Clinical presentation	Neck pain	Headache, gait instability	Neck pain	Neck pain	Diminution of vision	Neck pain, weakness limbs	Headache, proptosis, loss of vision		Neck swelling	Nasal obstruction, proptosis	
Duration (months)	8-9	6	18	4	5	3	8	8	3	4	6
Site	Clivus	Clivus	Clivus	Clivus	Clivus	Clivus	Clivus		Neck	Rt nasal	
Architecture	Solid	Lobular	Solid	Lobular	Lobular	Solid	Solid	Solid	Solid	Lobular	Lobular
Cellularity	C	N	C	N	N	C	C	C	C	N	N
Stroma	S	A	S	A	A	S	S	S	S	A	A
Mitoses/10 hpf	3–4	0–1	4	2	0–1	2–3	9	9–10	2	0–1	0–1
Necrosis (%)	+(40)	−	+(30)	+(40)	−	+(30)	−	+(30)	−	−	−
Vascular invasion	−	−	−	−	−	+	−	−	−	−	−
Cytologic atypia	+(vn)	−	+(vn)	+(sh)	+(sh)	+(vn)	+(vn)	+(vn)	+(vn)	−	−
Category	PD	Conv	Atyp	Conv	Conv	Atyp	Atyp	Atyp	Atyp	Conv	Conv
P53	+	−	+	−	+	+	+	+	+	+	+
INI1 IHC	−	−	−	−	+	−	−	−	−	+	+
INI1 FISH	loss	No tissue	No tissue	loss	Not done	Loss	loss		No tissue	Not done	
INI1 Sequencing	No mut	No tissue	No tissue	No mut	Not done	No mut	No mut		No tissue	Not done	
MIB-1 LI (%)	5	2	6	3	2	7–8	12–13	15	4	3	2
EGFR	+	+	+	+	+	+	+	+	+	+	+
Follow up	SD for 2mths and lost thereafter	SD 75 mths	NA	Expired	SD 57 mths	Expired	Recurrence at 3 mths, SD for 3 mths and lost thereafter		Expired	Recurrence at 4 mths & SD 16 mths	

Abbreviations: A, abundant; Atyp, atypical; C, hypercellular; Conv, conventional, F; female; IHC, immunohistochemistry; Lt, left; M, male; mths, months; mut, mutation; N, normocellular; NA, not available; PD, poorly differentiated; Recc, recurrent; Rt, right; S, scant; SD, stable disease; sh, smudgy hyperchromatic; vn, vesicular chromatin with nucleoli.
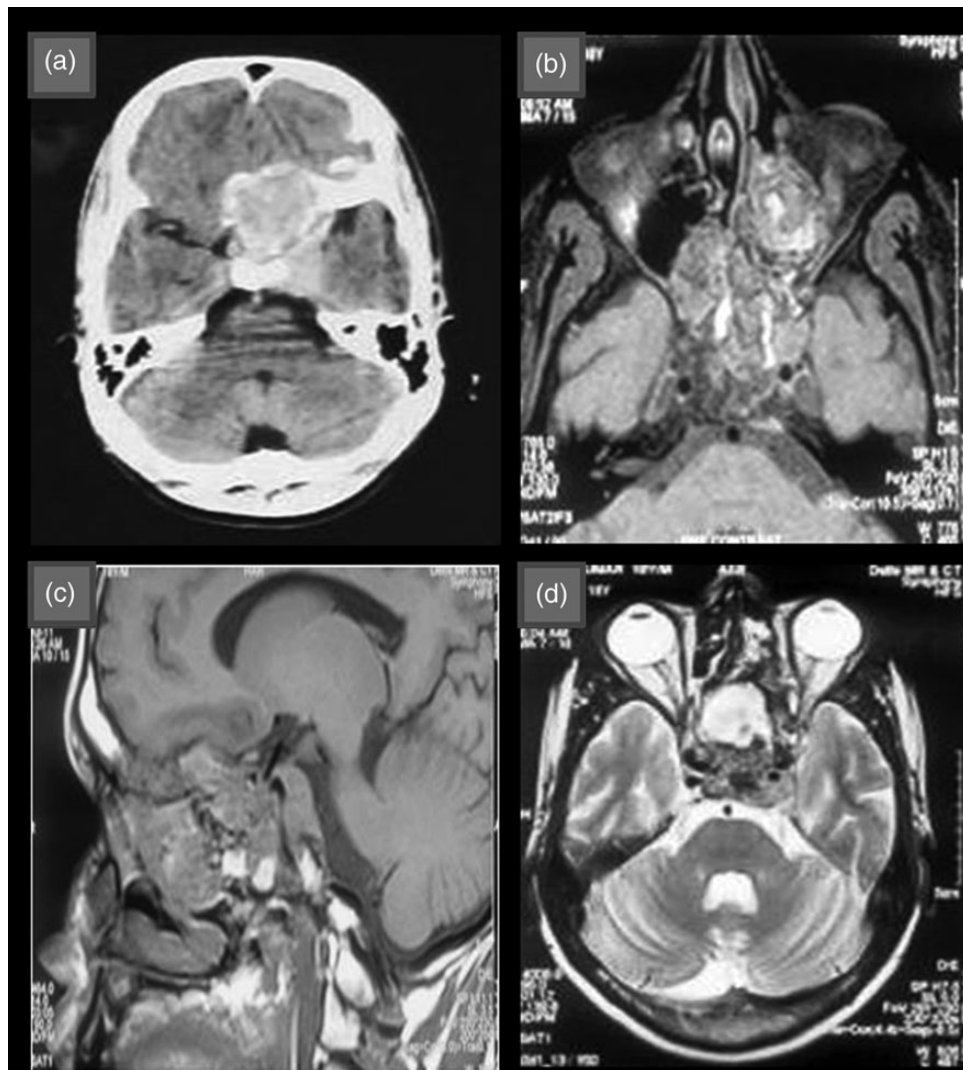
Fig. 1. (a) Contrast-enhanced computed tomographic image showing suprasellar space-occupying lesion with heterogenous contrast enhancement. (b) and (c) T1 weighted magnetic resonance image showing iso to hypointense lesion in suprasellar region with foci of high-signal intensity and extension to left orbit and ethmoid sinus. (d) T2 weighted magnetic resonance image showing hyperintense lesion in suprasellar region.

tomography and heterogenous enhancement on contrast injection. Bone erosion and bone destruction were also observed along with calcification (Fig. 1a). On T1-weighted magnetic resonance images, chordomas were iso or hypointense (Fig. 1b and c) and were hyperintense on T2-weighted images (Fig. 1d). None of the patients had metastasis.

Histopathological Features

Four tumors exhibited the features of conventional chordoma. These were characterized by lobulated architecture, abundant myxoid matrix, and low cellularity (Fig. 2a). Tumor cells were arranged in cords, strands, and cohesive clusters (Fig. 2b). The tumor cells were large, polygonal, and contained abundant eosinophilic to amphophilic cytoplasm with round clear vacuoles in some (Fig. 2c). Nuclei ranged from small and hyperchromatic to large and vesicular. One case showed marked cytoplasmic vacuolization,

making it resemble mature adipocytes (lipoid appearance) (Fig. 2d).

Four tumors were highly cellular and showed a solid growth pattern, with tumor cells arranged in confluent sheets, minimal/no intervening myxoid matrix, and/or diffuse cytologic atypia with enlarged nuclei, vesicular chromatin, and prominent nucleoli or small smudged hyperchromatic nuclei (Fig. 3a and b). Physaliferous cells ranged from none to few. These tumors were included in the cellular/atypical chordoma group. One tumor showed moderate acute and chronic inflammation and evidence of old hemorrhage. The third group of poorly differentiated chordomas consisted of one tumor, which was characterized by sheets of epithelioid cells with increased nuclear-cytoplasmic ratio, oval-irregular nuclei, and minimal eosinophilic-to-clear cytoplasm (Fig. 3c and d). Tumor cells showed spindling in some areas and interspersed neutrophilic sprinkling. This tumor resembled poorly differentiated carcinoma/sarcoma.
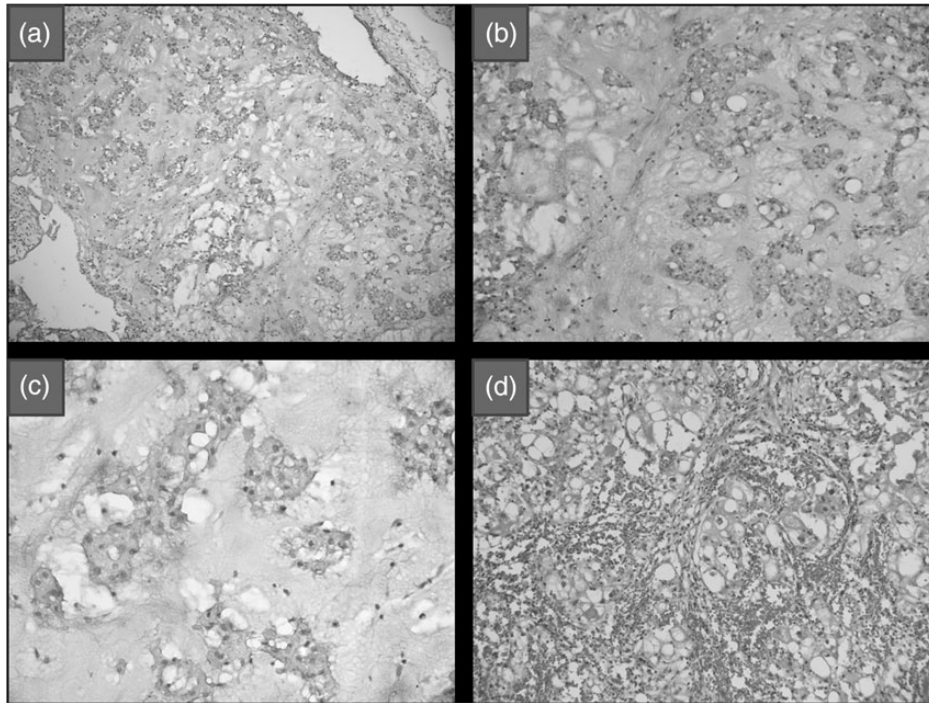
Fig. 2. (a) Conventional chordoma with lobulated architecture, abundant myxoid matrix, and low cellularity (hematoxylin and eosin [H&E], X100). (b) Tumor cells arranged in cords, strands, and cohesive clusters (H&E, X200). (c) Large polygonal cells with abundant eosinophilic to amphophilic cytoplasm and small nuclei (H&E, X400). (d) Tumor cells with marked cytoplasmic vacuolization resembling mature adipocytes (lipoid) (H&E, X200).
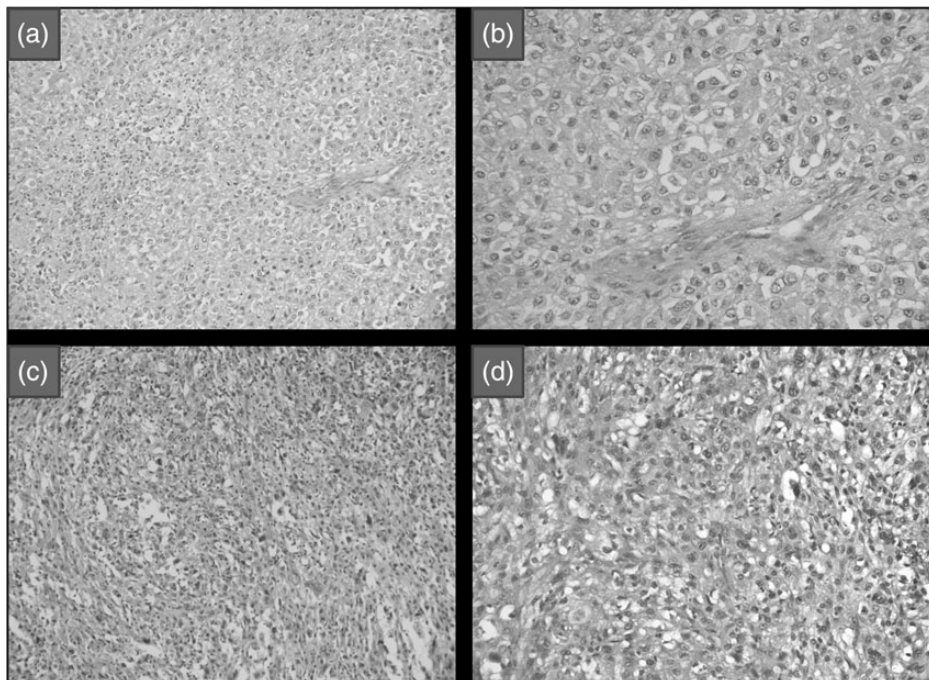

Fig. 3. (a) Atypical chordoma showing high cellularity and a solid growth pattern with tumor cells arranged in confluent sheets and no intervening myxoid matrix (hematoxylin and eosin [H&E],X200. (b) Diffuse cytologic atypia with enlarged nuclei and vesicular chromatin in atypical chordoma (H&E, X200). (c) Poorly differentiated chordoma showing sheets of epithelioid cells with focal spindling (H&E, X400). (d) Tumor cells with increased nuclear cytoplasmic ratio, oval-irregular nuclei, minimal eosinophilic-to-clear cytoplasm, and frequent mitoses in poorly differentiated chordoma (H&E, X400).

Cytologic atypia was absent in 2 conventional chordomas and minimal in the other 2 (Table 2). Diffuse cytologic atypia was observed in all atypical and poorly differentiated chordomas. Chondroid differentiation was not observed in any tumor. One of the atypical chordomas showed vascular emboli. Necrosis was seen in one conventional, 3 atypical, and one poorly differentiated chordoma. The percentage of necrosis ranged from 30%–40% but was more frequently found in atypical and poorly differentiated chordomas.

Mitotic activity was present in all 3 groups; mitotic count was <2/10 hpf (0–1) in conventional chordomas, varied from 2–10/10 hpf in the atypical group, and was 4/10 hpf in the poorly differentiated chordoma. MIB-1 LI ranged from 2%–3% in conventional, 5%–15% in atypical (Fig. 4a), and 5% in the poorly differentiated chordoma.

Immunohistochemical Profile

All tumors showed expression of CK, EMA, vimentin, S 100, and brachyury (100%) (Fig. 4b and c). Seven tumors showed p53 expression (77.7%) (Fig. 4d). Two conventional chordomas did not show p53 expression. INI1 expression was absent in 7 tumors (77.7%). Only 2 conventional chordomas showed INI1 expression. EGFR expression was seen in all tumors (100%). None of the tumors with atypical morphology showed expression of desmin, GFAP, synaptophysin, chromogranin, and smooth muscle actin (SMA). CD117 expression was not noted in any of the tumors. Only 2 AT/RTs of brain showed focal nuclear expression for brachyury, as compared with chordomas, in which it was diffuse and strong. The remaining 3 renal rhabdoid tumors and 13 central nervous AT/RTs did not show brachyury expression.

Table 2. Comparison of histomorphological features and MIB-1 LI score amongst conventional, atypical, and poorly differentiated pediatric chordomas

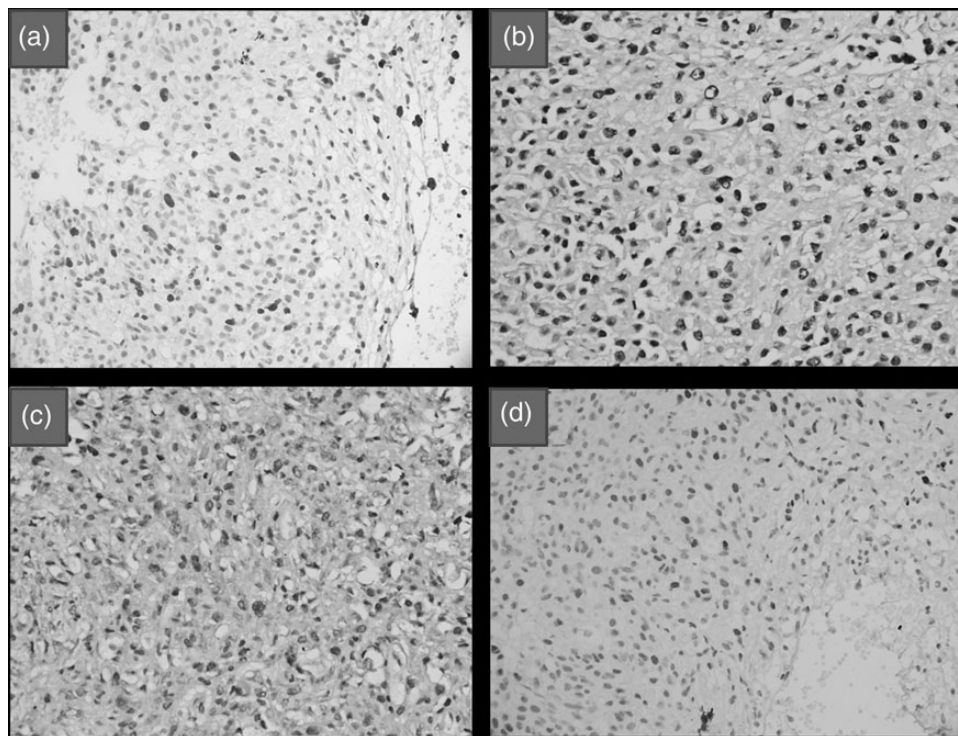| Feature	Number of cases- 9		
	Conventional(4)	Atypical(4)	Poorly Differentiated(1)
Cytologic atypia	2/4 (50% & minimal)	4/4 (100% &diffuse)	1/1 (100% &diffuse)
Necrosis	1/4 (25%)	3/4 (75%)	1/1 (100%)
Mitoses/10 hpf	0-1	2-10	4
MIB1-LI score 1	0/4 (0%)	4/4 (100%)	1/1 (100%)

Fig. 4. Atypical chordoma showing (a) high MIB1 LI and (b) brachyury expression. (c) Expression of brachyury in a case of poorly differentiated chordoma. (d) p53 expression in an atypical chordoma X400 [Immunohistochemical stains].

DNA Sequencing

None of the 5 tumors subjected to DNA sequencing showed mutations in INI1 gene in any of the 9 exons.

Fluorescent in Situ Hybridization

FISH analysis carried out in 4 childhood chordomas with INI1 loss showed loss of INI1 locus. One of the 5 adult chordomas also showed this loss.

Follow-up

Out of 9 pediatric patients, one did not return for follow-up, and 3 patients expired. Amongst the 3 patients who expired, 2 were diagnosed with atypical chordoma. One of these 2 patients was a 2-year-old female who died within a few days of diagnosis before any treatment could be administered. The tumor involved prevertebral and paravertebral spaces and extended to both carotid spaces with involvement of the nasopharynx and evidence of intraspinal extension. The second patient was a 6-year-old male who was operated and diagnosed to have atypical chordoma. He died in the postoperative period in-hospital stay due to post-operative infection and respiratory failure. The third patient was a 10-year-old male who was operated and diagnosed to have conventional chordoma. He was recommended adjuvant radiation and chemotherapy but deferred the same and died 3 months following surgery. Another patient, an 18-year-old male who was operated and diagnosed with atypical chordoma, presented with recurrence 3 months later. He was reoperated, advised adjuvant radiotherapy, and was on regular follow-up for 3 months only. One patient, who was diagnosed with poorly differentiated chordoma, received adjuvant radiotherapy and was on follow-up for 2 months only. Three patients with conventional chordoma are on regular follow-up at 75, 57, and 20 months respectively. One of them had a recurrence, was reoperated, and administered adjuvant imatinib therapy for one year. All 3 of them have residual stable disease and are asymptomatic.

Adult Group

For comparison, 13 adult chordomas were included in the study, of which 6 were recurrent. Ages of the patients ranged from 26–70 years with a mean age of 45.5 years. The group comprised 12 males and one female. Sacrococcygeal, lumbar, clivus, petroclivus, and ethmoid were the locations. Headache, pain in the back or lower limbs, alteration of voice, nasal regurgitation, constipation, urinary retention, dysphagia, and facial nerve palsy were the presenting symptoms and signs.

All tumors showed the histopathological features of conventional chordoma. No tumor showed vascular invasion, chondroid, atypical, or poorly differentiated morphology. Cytologic atypia was seen in 3 recurrent tumors, but it was focal (Tables 3 and 4). Necrosis was seen in 3 nonrecurrent and 2 recurrent chordomas. In all 5 tumors, the percentages of necrosis were <20%. Mitotic count was ≤2/10 hpf in 6 and 4/10 hpf in one nonrecurrent chordoma. In the recurrent group, it ranged from 0–4/10 hpf. MIB-1 LI was <5% in all nonrecurrent tumors, while it was ≥5% in half of the recurrent tumors. Three adult chordomas showed lipoid differentiation. All tumors showed expression of CK, EMA, S100, and vimentin. P53 expression was seen in 4 tumors (30.7%), of which 2 were recurrent. EGFR expression was noted in all chordomas whereas one (7.6%) showed INI1 loss.

Discussion

Chordomas are rare neoplasms that arise from persistent notochord tissue. These tumors can arise anywhere along the axial spine but are most commonly seen in the skull base/clivus and sacrococcygeal regions.[11,12] These tumors occur most often in people in their 40's and 50's and very rarely occur in infancy and childhood. The reported male preponderance is also noted in the present series, both in adults as well as in children. The sacrococcygeal region is the common location in adults, whereas base of skull is more common in children and adolescents.[13,15,16] Symptoms depend on the location of lesion and are the result of mass effect. Although typically slow-growing, chordomas are extremely difficult to eradicate by surgical and adjuvant therapy. Multiple recurrences are frequent, resulting in considerable morbidity and mortality. Five- and 10-year survival rates vary from 70% to 80% and 30% to 40%, respectively.[11] Chordomas in children and adolescents are uncommon and account for <5% of all chordomas.[17] In general, younger patients have improved overall survival as compared with adults, but a subset of pediatric chordomas shows atypical histology and aggressive behavior.[9] The data and

Table 3. Histopathologic and immunohistochemical differences between pediatric and adult chordomas

Feature	Number of cases	
	Pediatric (9)	Adult (13)
Cytologic atypia	7/9 (77.7%, diffuse)	3/13 (23.0%, focal)
Necrosis	5/9 (55.5%)	5/13 (38.4%)
Mitoses/10 hpf(>2)	5/9 (55.5%)	3/13 (23.0%)
MIB-1 LI score 1	5/9 (55.5%)	3/13 (23.0%)
P53	7/9 (77.7%)	4/13 (30.7%)
INI1 loss	7/9 (77.7%)	1/13 (7.6%)
EGFR	9/9 (100%)	13/13 (100%)

Table 4. Comparison of histomorphological features MIB-1 LI score amongst recurrent and nonrecurrent adult chordomas

Feature	Number of cases-13	
	Recurrent(6)	Nonrecurrent(7)
Cytologic atypia	3/6 (50%, focal)	0/7 (0%)
Necrosis	2/6 (33.3%)	3/7 (42.8%)
Mitoses/10 hpf		
≤2	4/6 (66.6%)	6/7 (85.7%)
>2	2/6 (33.3%)	1/7 (14.2%)
MIB-1 LI score 1	3/6 (50%)	0/7 (0%)

experience with their clinicopathologic features and immunohisto-chemical profiles are limited due to their rarity. Fewer than 100 cases of skull base chordomas occurring in children and adolescents have been reported in the literature, and most of them have been described as isolated cases.[18–24] Most of these childhood chordomas had more aggressive behavior and metastasized more frequently than in adults. There are a very few large case series of pediatric chordomas. Coffin et al reported 12 cases of pediatric chordomas in patients <20 years of age. Half of the cases arose in the clivus and had atypical morphology. Metastasis occurred in 7 cases, and 10 patients died of disease in the follow-up period, which ranged from 3 weeks to 4.5 years.[13] Borba et al reviewed 79 cases of spheno-occipital chordoma in patients < 20 years of age. Classical, chondroid, and atypical cases constituted 64.6%, 13.5% , and 22.4% with mortality of 23.1%, 37.5%, and 100%, respectively. They postulated that adjuvant radiation therapy resulted in better overall survival than surgery alone.[9] Wold and Laws studied 12 cases of skull base chordomas in patients <20 years of age at Mayo Clinic. Six cases showed chondroid morphology, and there were no cases with unusual histologic features. All patients were treated with surgery and postoperative radiation. Two patients died of disease. These authors advocated surgery with radiation for better survival.[17] Hoch and colleagues examined a series of 73 children and adolescents (Age range: 1–18 years) with skull base chordomas. Conventional, chondroid, atypical, and poorly differentiated cases constituted 58%, 23%, 11%, and 8% with mortality rates of 14%, 18%, 0%, and 83%, respectively. One patient with poorly differentiated chordoma died of disease. They concluded that base-of-skull chordomas treated with proton beam radiation have better survival than in adults. However, poorly differentiated chordomas are highly aggressive tumors.[8] Robert et al examined the clinical and histologic features of 35 cases of chordomas in young patients (<25 years old). There were 13 deaths (37%), and 3 patients had metastasis during an average follow-up period of 129 months. Survival rate was slightly better than the reported mortality rate for adults, but there was a subset of young patients with atypical morphology who had a significantly worse survival rate, suggesting that histologic subtyping may be predictive of prognosis.[10] Interestingly, none of the tumors in the present series showed chondroid differentiation. The current series emphasizes that atypical morphology, coupled with high MIB-1 LI, is commonly seen in childhood chordomas and is an indicator of worse prognosis.

INI1 (SMARCB1) is a member of the ATP-dependent SWI/SNF chromatin-remodeling complex, and it is thought to function as a tumor suppressor gene.[25] It is located on chromosome 22q11.2, is normally expressed in all tissues, and plays an important role in differential diagnosis of pediatric central nervous system tumors. Loss of INI1 was originally believed to be specific to atypical teratoid/rhabdoid tumors (AT/RT) and extrarenal malignant rhabdoid tumors.[26] Recently, among neural tumors, cribriform neuroepithelial tumor, primitive neuroectodermal tumor, and schwannomatosis have been associated with INI1 loss.[27,28] Moreover, loss of INI1 expression has also been discovered in extra-neural tumors including epithelioid sarcoma, synovial sarcoma, epithelioid malignant peripheral nerve sheath tumor, myoepithelial carcinoma, and renal medullary carcinoma.[29–33] Pediatric central nervous system tumors negative for INI1 tend to show an aggressive course even if they lack rhabdoid features.[26] Mobley et al noted loss of INI1 in 3 of 4 cases of poorly

differentiated chordomas, but none of them revealed point mutations on DNA sequencing.[2] In our study, 77.7% of pediatric chordomas showed loss of INI1 as compared with 7.6% in adults. Loss of the INI1 (SMARCB1) locus by FISH was noted in all 4 cases of childhood chordomas but in only one of the adult chordomas studied. We did not find any mutation in all 9 coding exons of INI1 gene in tumors that did not show INI1 expression on IHC. Our results were similar to the earlier reported findings.[2] Similar results have also been reported in a subgroup of rhabdoid tumors and epithelioid sarcomas where patients with protein loss had no mutation in INI1 gene.[34–36] The possible explanation for this discrepancy is that inactivation of INI1 in rhabdoid tumors may be attributable to posttranscriptional or posttranslational modifications that are not detectable by sequencing or FISH. It is also hypothesized that alternatively a second locus for rhabdoid tumor development may play a role in absence of INI1 protein with no detectable mutation at INI1 gene level. It may also be possible that some epigenetic events may be responsible for loss of protein expression without genomic instability, as speculated earlier, and partly shown that epigenetic alterations are the main driving force behind the initiation and progression of multiple cancers.[37,38] Therefore, it is possible that molecular alterations in childhood chordomas are different from adult chordomas and could be responsible for their sinister prognosis. Although histomorphologic features of chordomas are characteristic, atypical morphology in children poses a difficulty in the diagnosis, and these tumors maybe misdiagnosed as poorly differentiated carcinomas or sarcomas. In such situations, loss of INI1 is a valuable diagnostic tool. In addition, brachyury expression helps in distinguishing atypical and poorly differentiated chordomas from AT/RT and poorly differentiated carcinoma/sarcoma.[39] Furthermore, AT/RTs show variable expression of GFAP, synaptophysin, chromogranin, neurofilament, and SMA, whereas chordomas uniformly show S100 expression with absence of SMA, GFAP, and synaptophysin expression. Although clivus is a rare site of occurrence for rhabdoid tumors in children, these tumors definitely pose a diagnostic challenge for differentiation from childhood chordomas.[40] This is further complicated by loss of INI1 expression in both of these tumors; however, brachyury is helpful in differentiating between the 2 because it is either absent or only very focally present in AT/RTs. Alternatively, it may be possible that some of these childhood chordomas with atypical features are actually AT/RTs, as they show loss of INI1 and behave more aggressively like AT/RTs. TP53 is a critical regulator of cell cycle, and a large number of human neoplasms show some alteration of the p53 protein. In a study conducted by Horbinsky et al, 44% cases of skull base chordomas showed p53 accumulation.[12] We found p53 expression in 77.7% and 30.7% of pediatric and adult cases, respectively. Thus, pediatric chordomas show p53 expression more frequently than adult cases. The mainstay of treatment of chordomas is excision. Adjuvant proton therapy is given following surgery for base-of-skull tumors. Currently, there is no effective drug therapy for treating chordomas; however, there is evidence that some patients respond to the empirical use of epidermal growth factor receptor antagonists.[41] Shalaby et al studied the role of EGFR in pathogenesis of chordoma by IHC, FISH, and sequencing. They implicated aberrant EGFR signaling in the pathogenesis of chordoma.[3] EGFR expression was noted in all cases, suggesting that EGFR may serve as an important therapeutic target in cases that are refractory to conventional treatment.

Conclusion

Although chordomas in children and adolescents are rare, the possibility should be considered in skull-base tumors. A subset of chordomas with atypical histomorphologic features (atypical and poorly differentiated) needs to be identified because they behave in an aggressive manner and require adjuvant therapy. Pediatric chordomas are different from those that occur in adults as they show p53 expression, INI1 loss, and higher MIB-1 LI; however, EGFR expression is common to both.

Conflict of interest statement. None declared.

References

1. Heffelfinger MJ, Dahlin DC, MacCarty CS, et al. Chordomas and cartilaginous tumors at the skull base. *Cancer*. 1973;32(2):410–420.

2. Mobley BC, McKenney JK, Bangs CD, et al. Loss of SMARCB1/INI1 expression in poorly differentiated chordomas. *Acta Neuropathol*. 2010;120(6):745–753.

3. Shalaby A, Presneau N, Ye H, et al. The role of epidermal growth factor receptor in chordoma pathogenesis: a potential therapeutic target. *J Pathol*. 2011;223(3):336–346.

4. Zhou H, Chen CB, Lan J, et al. Differential proteomic profiling of chordomas and analysis of prognostic factors. *J Surg Onc*. 2010; 102(7):720–727.

5. Deshpande V, Nielsen GP, Rosenthal DI, et al. Intraosseous benign notochord cell tumors (BNCT): further evidence supporting a relationship to chordoma. *Am J Surg Pathol*. 2007;31(10):1573–1577.

6. Yamaguchi T, Yamato M, Saotome K. First histologically confirmed case of a classic chordoma arising in a precursor benign notochordal lesion: differential diagnosis of benign and malignant notochordal lesions. *Skeletal Radiol*. 2002;31:413–418.

7. Tos APD. Unveiling the molecular pathogenesis of chordoma: a new paradigm for molecular targeting of rare cancers. *J Pathol*. 2011; 223(5):565–566.

8. Hoch BL, Nielsen GP, Liebsch NJ, Rosenberg AE. Base of skull chordomas in children and adolescents: a clinicopathologic study of 73 cases. *Am J Surg Pathol*. 2006;30(7):811–818.

9. Borba LA, Al-Mefty O, Mrak RE, Suen J. Cranial chordomas in children and adolescents. *J Neurosurg*. 1996;84(4):584–591.

10. Ridenour RV, Ahrens WA, Folpe AL, Miller DV. Clinical and histopathologic features of chordomas in children and young adults. *Pediatric and Developmental Pathology*. 2010;13(1):9–17.

11. Yoneoka Y, Tsumanuma I, Fukuda M, et al. Cranial base chordoma— long term outcome and review of the literature. *Acta Neurochir (Wien)*. 2008;150(8):773–778.

12. Horbinski C, Oakley GJ, Cieply K, et al. The prognostic value of ki-67, p53, epidermal growth factor receptor, 1p36, 9p21, 10q23, and 17p13 in skull base chordomas. *Arch Pathol Lab Med*. 2010;134(8):1170–1176.

13. Coffin CM, Swanson PE, Wick MR, et al. Chordoma in childhood and adolescence: a clinicopathologic analysis of 12 cases. *Arch Pathol Lab Med*. 1993;117(9):927–933.

14. Kraus JA, de Millas W, Sörensen N, et al. Indications for a tumor suppressor gene at 22q11 involved in the pathogenesis of ependymal tumors and distinct from hSNF5/INI1. *Acta Neuropathol*. 2001;102(1):69–74.

15. Seung WB, Kim SM. Clival cystic chordoma in children with confused magnetic resonance imaging. *J Korean Neurosurg Soc*. 2004;36: 422–424.

16. Handa J, Suzuki F, Nioka H, Koyama T. Clivus chordoma in childhood. *Surg Neurol*. 1987;28(1):58–62.

17. Wold LE, Laws ER. Cranial chordomas in children and young adults. *J Neurosurg*. 1983;59(6):1043–1047.

18. Sassin JF, Chutorian AM. Intracranial chordoma in children. *Arch Neurol*. 1967;17(1):89–93.

19. Becker LE, Yates AJ, Hoffman HJ, et al. Intracranial chordoma in infancy: case report. *J Neurosurg*. 1975;42(3):349–352.

20. Nolte K. Malignant intracranial chordoma and sarcoma of the clivus in infancy. *Pediatr Radiol*. 1979;8(1):1–6.

21. Sibley RK, Day DL, Dehner LP. Metastasizing chordoma in early childhood: a pathological and immunohistochemical study with review of the literature. *Pediatr Pathol*. 1987;7(3):287–301.

22. Chetty R, Levin CV, Kalan MR. Chordoma: a 20 year Clinicopathologic review of the experience at Groote Schuur Hospital, Cape Town. *J Surg Oncol*. 1991;46(4):261–264.

23. Kaneko Y, Sato Y, Iwaki T, et al. Chordoma in early childhood: a clinicopathological study. *Neurosurgery*. 1991;29(3):442–446.

24. Yadav YR, Kak VK, Khosla VK, et al. Cranial chordoma in the first decade. *Clin Neurol Neurosurg*. 1992;94(3):241–246.

25. Versteege I, Sevenet N, Lange J, et al. Truncating mutations of hSNF5/ INI1 in aggressive pediatric cancer. *Nature*. 1998;394(6689):203–206.

26. Judkins AR, Mauger J, Rorke LB, Biegel JA. Immunohistochemical analysis of hSNF5/INI1 in pediatric CNS neoplasms. *Am J Surg Pathol*. 2004;28(5):644–650.

27. Hasselblatt M, Oyen F, Gesk S. Cribriform neuroepithelial tumor (CRINET): a nonrhabdoid ventricular tumor with INI1 loss and relatively favorable prognosis. *J Neuropathol Exp Neurol*. 2009;68(12): 1249–1255.

28. Hulsebos TJM, Plomp AS, Wolterman RA, et al. Germline mutation of INI1/SMARCB1 in familial Schwannomatosis. *Am J Hum Genet*. 2007; 80(4):805–810.

29. Hornick JL, Dal Cin P, Fletcher CD. Loss of INI1 expression is characteristic of both conventional and proximal type epithelioid sarcoma. *Am J Surg Pathol*. 2009;33(4):542–550.

30. Kohashi K, Oda Y, Yamamoto H, et al. Reduced expression of SMARCB1/ INI1 protein in synovial sarcoma. *Mod Pathol*. 2010;23(7):981–990.

31. Carter JM, O'Hara C, Dundas G, et al. Epithelioid malignant peripheral nerve sheath tumor arising in a schwannoma, in a patient with "Neuroblastoma-like" schwannomatosis and a novel germline SMARCB1 mutation. *Am J Surg Pathol*. 2012;36(1):154–160.

32. Gleason BC, Fletcher CD. Myoepithelial carcinoma of soft tissue in children: an aggressive neoplasm analyzed in a series of 29 cases. *Am J Surg Pathol*. 2007;31(12):1813–1824.

33. Cheng JX, Tretiakova M, Gong C, et al. Renal medullary carcinoma: rhabdoid features and the absence of INI1 expression as markers of aggressive behavior. *Mod Pathol*. 2008;21(6):647–652.

34. Sigauke E, Rakheja D, Maddox DL, et al. Absence of expression of SMARCB1/INI1 in malignant rhabdoid tumors of the central nervous system, kidneys and soft tissue: an immunohistochemical study with implications for diagnosis. *Mod Pathol*. 2006;19(5):717–725.

35. Kohashi K, Oda Y, Yamamoto H, et al. SMARCB1/INI1 protein expression in round cell soft tissue sarcomas associated with chromosomal translocations involving EWS: a special reference to SMARCB1/INI1 negative variant extraskeletal myxoid chondrosarcoma. *Am J Surg Pathol*. 2008;32(8):1168–1174.

36. Kohashi K, Izumi T, Oda Y, et al. Infrequent SMARCB1/INI1 gene alteration in epithelioid sarcoma: a useful tool in distinguishing epithelioid sarcoma from malignant rhabdoid tumor. *Hum Pathol*. 2009;40(3):349–355.

37. Zhang F, Tan L, Wainwright LM, Bartolomei MS, Biegel JA. No evidence for hypermethylation of the hSNF5/INI1 promoter in pediatric rhabdoid tumors. *Genes Chromosomes Cancer*. 2002;34(4):398–405.

38. McKenna ES, Roberts CW. Epigenetics and cancer without genomic instability. *Cell Cycle*. 2009;8(1):23–26.

39. Vujovic S, Henderson S, Presneau N, et al. Brachyury, a crucial regulator of notochordal development, is a novel biomarker for chordomas. *J Pathol*. 2006;209(2):157–165.

40. Kazan S, Göksu E, Mihci E, Gökhan G, Keser I, Gürer I. Primary atypical teratoid/rhabdoid tumor of the clival region. *Case report. J Neurosurg*. 2007;106(4):308–311.

41. Linden O, Stenberg L, Kjellen E. Regression of cervical spinal cord compression in a patient with chordoma following treatment with cetuximab and gefitinib. *Acta Oncol*. 2009;48(1):158–159.